Application of Ampere's force law to railgun accelerators

Peter Graneau

Citation: J. Appl. Phys. **53**, 6648 (1982); doi: 10.1063/1.330097
View online: http://dx.doi.org/10.1063/1.330097
View Table of Contents: http://jap.aip.org/resource/1/JAPIAU/v53/i10
Published by the AIP Publishing LLC.

Application of Ampere's force law to railgun accelerators

Peter Graneau
Massachusetts Institute of Technology, Francis Bitter National Magnet Laboratory, Cambridge, Massachusetts 02139

(Received 2 September 1981; accepted for publication 22 June 1982)

This paper examines the question of where in the railgun accelerator circuit is the seat of the recoil force. It is explained that conventional electromagnetic field theory and the older Ampere electrodynamics disagree on this point. The former places the recoil force in the remote gun breach while the latter claims it resides in the railheads close to the projectile. An experiment is described which tends to confirm the Ampere prediction. The second part of the paper deals with the force distribution along the projectile branch of the accelerator. Finite current-element analysis has been employed to show that both theories give approximately the same acceleration force distribution and that the total acceleration force furnished by them agrees well with an experimental check. However, according to the Ampere law, the projectile branch of the circuit should also be subject to strut compression and not only to transverse acceleration. This aspect of the Ampere electrodynamics still awaits experimental confirmation.

PACS numbers: 41.10. – j, 84.90. + a

I. INTRODUCTION

Railguns are an old concept for the linear acceleration of metallic conductors bridging a pair of rails which form a go-and-return circuit. Sliding metallic contacts and arcs have been used to transfer the current between rails and the projectile. Both alternating and direct currents will drive railguns but dc is less wasteful in Joule heating. References 1–5 describe interest in this type of accelerator for a variety of applications from macroparticle impact nuclear fusion to space launchers.

Figure 1 serves to explain railgun terminology. It also provides a qualitative picture of the Lorentz force distribution around a rectangular circuit. The projectile, or payload, has to be rigidly attached to the p branch of the circuit which contacts the rails at A and B. The acceleration force on p is denoted by F_a. An equal and opposite force F_b acts on b. The b branch is often referred to as the gun breach. This latter branch of the circuit must include the power source.

The purpose of the paper is to ponder two unresolved questions which are of practical importance to the design of railgun accelerators. The first one asks where in the stationary rails s and t or the breach b of the railgun does the recoil force arise. The second question addresses the force distribution along the projectile branch of the accelerator. Two experiments are outlined which support predictions made by the now little-known electrodynamic force law first proposed by Ampere.

II. AVAILABLE FORCE LAWS

Most investigators[2–7] of reaction forces between parts of a circuit have calculated the acceleration force with

$$F_a = (1/2)(dL/dx)i^2, \tag{1}$$

where dL is the change in self-inductance of the rectangular circuit for a virtual displacement dx of the p branch in the direction of F_a. Two disadvantages of this formula are that it does not give the force distribution, nor does it define the seat of the recoil force. Maxwell[8] appears to have been first in pointing out that Eq. (1) agrees with Ampere's force law which is

$$\Delta F_{m,n} = -i^2(dm.dn/r_{m,n}^2)(2\cos\epsilon - 3\cos\alpha\cos\beta), \tag{2}$$

where $i.dm$ and $i.dn$ are two current elements of the same circuit inclined to each other by the angle ϵ, while α and β are the inclinations of the elements to the distance vector $r_{m,n}$, as shown in Fig. 2. $\Delta F_{m,n}$ is an elemental force of repulsion (positive) or attraction (negative). Maxwell[8] provided proof of the agreement between Eqs. (1) and (2) for two parallel wires carrying current in opposite directions.

With the introduction of special relativity, Ampere's force law was dropped in favor of the Biot-Savart-Lorentz force law first suggested by Grassmann [9] This takes the form

$$\Delta\mathbf{F}_m = (i^2/r_{m,n}^2)\mathbf{dm}\times(\mathbf{dn}\times\mathbf{1}_r),$$
$$\Delta\mathbf{F}_n = (i^2/r_{m,n}^2)\mathbf{dn}\times(\mathbf{dm}\times\mathbf{1}_r), \tag{3}$$

where $\Delta\mathbf{F}_m$ is the elemental vector force on element $i.dm$ and $\Delta\mathbf{F}_n$ the corresponding force on element $i.dn$. The unit distance vector $\mathbf{1}_r$ has to be drawn in the direction of the line connecting the two elements and must point toward the element at which the force is being determined. It is obvious that Eqs. (2) and (3) disagree on the direction and magnitude of elemental interaction forces, but this disagreement does not necessarily carry over to the total reaction forces between parts of a circuit. Maxwell, for example, was of the opinion that they would give the same total reaction forces whatever the circuit geometry. Not having computers at his disposal, he was unable to check this opinion. The voluminous literature on electromagnetism does not appear to provide an analytical method of calculating reaction forces in arbitrarily shaped circuits from either Eq. (2) or (3).

All three laws give the force in dyne if the current is expressed in absolute ampere and the distance in centimeter ($1\,\mathrm{N} = 10^5$ dyn; $1\,\mathrm{A_{ab}} = 10\,\mathrm{A}$). It will be found convenient to define specific force as the actual force divided by the square of the current. The specific force is a dimensionless shape constant of the railgun accelerator.

Ampere's law, Eq. (2), and the Lorentz force law, Eq.

 0021-8979/82/106648-07$02.40

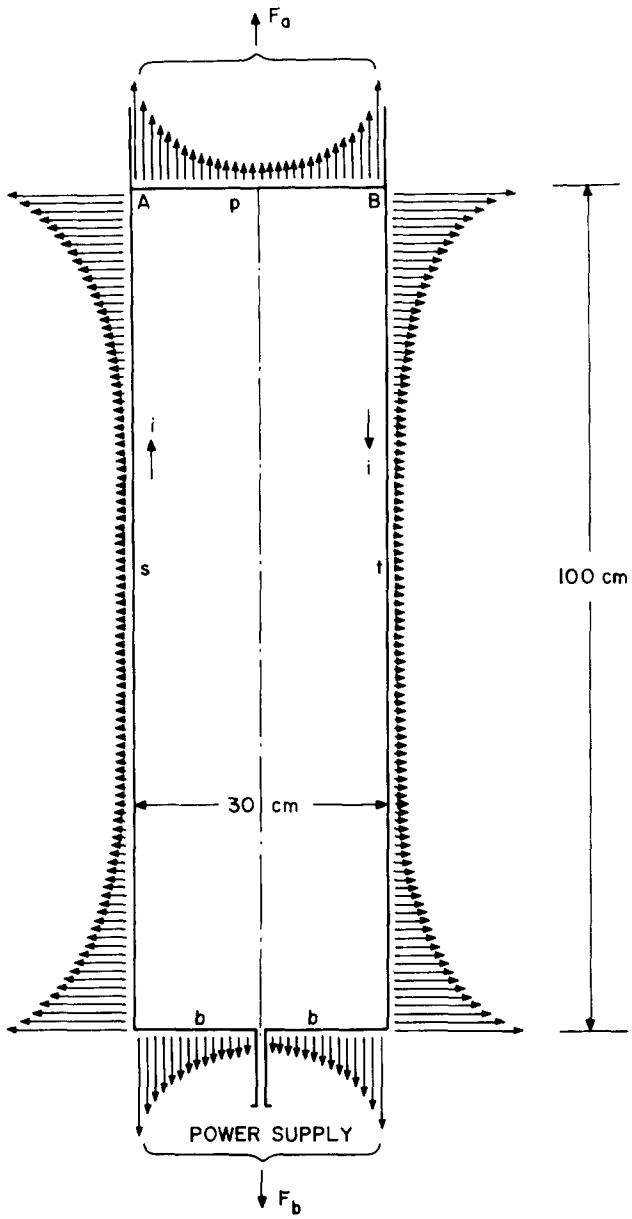

FIG. 1. Railgun circuit with Lorentz or transverse Ampere force distribution. The dimensions of the circuit have been chosen for the experiment described in Sec. VI.

(3), specify different positions in the stationary part of the railgun circuit at which the recoil force should be generated. This force is not localized by the self-inductance gradient formula, Eq. (1).

Ampere's interaction force between any two current elements of the rigidly connected body made up of *s*, *t*, and *b* of Fig. 1 will be a reciprocal repulsion or attraction which cannot contribute to the reaction force between *p* and the stationary part *s-t-b* of the circuit. Therefore, in order to determine the Ampere distribution of the reaction force in the rail and the breach, we need only sum elemental repulsions and attractions between element pairs of which one member resides in the *p* branch and the other in the remainder of the circuit. Vectorially summing the interactions of one element *i.dm* in *s-t-b* with all elements *i.dn* in *p* and resolving this sum along the direction of the acceleration force gives the recoil on *i.dm*. The distribution of the recoil

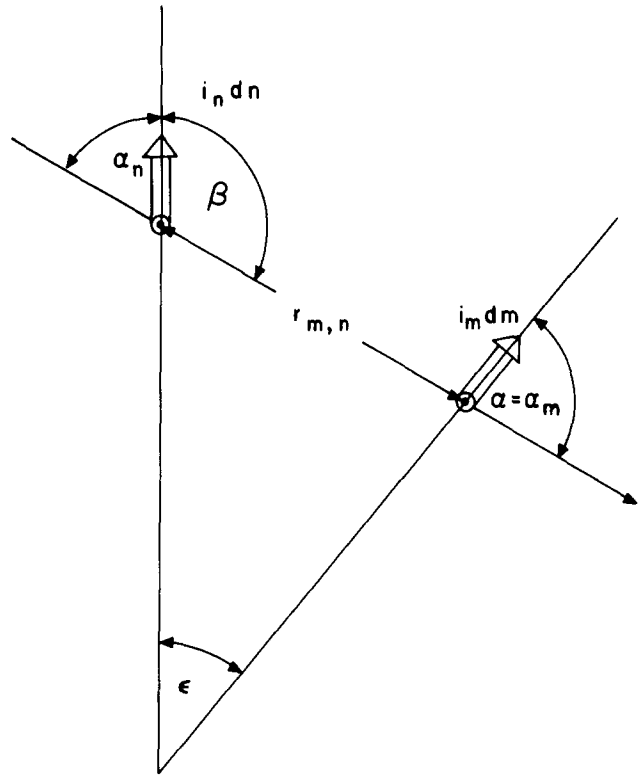

FIG. 2. Angle convention for the Ampere and Grassmann formulas [Eqs. (2) and (4)].

force is obtained by letting *i.dm* assume all possible positions in *s-t-b*.

When using the Biot-Savart-Lorentz force law, Eq. (3), the recoil force analysis becomes far more difficult. As we are then not dealing with reciprocal repulsions and attractions, the interaction of two current elements, both of which are located within *s-t-b*, can apparently make a contribution to the recoil force. Here it should be remembered that relativistic field theory does not conform with Newton's third law. In fact, according to conventional concepts, almost all the force F_b in Fig. 1 is due to the current in the rails and therefore arises from internal interactions inside *s-t-b*.

The triple vector product of Eq. (3) may be expanded to

$$\Delta \mathbf{F}_m = \mathbf{dn}(1/r_{m,n}^2) i^2\, dm \cos \alpha_m - \mathbf{1}_r (1/r_{m,n}^2) i^2\, dm\, dn \cos \epsilon,$$

$$\Delta \mathbf{F}_n = \mathbf{dm}(1/r_{m,n}^2) i^2\, dn \cos \alpha_n - \mathbf{1}_r (1/r_{m,n}^2) i^2\, dm\, dn \cos \epsilon. \quad (4)$$

This form of the Lorentz force law is suitable for finite current-element analysis by computer. The angles of Eq. (4) are defined by Fig. 2.

Now to compute the recoil force distribution on *s-t-b* we have to sum the interactions of *i.dm* with *all* remaining elements of the *whole* of the circuit, resolve this vector sum in the direction of the acceleration force F_a, and repeat the process for all possible positions of *i.dm* in *s-t-b*. But we know from the start that Lorentz forces on rail elements are perpendicular to F_a and therefore cannot contribute to the recoil. Hence we need only consider the positions of *i.dm* in the branch *b*. This will give the distribution of F_b indicated in Fig. 1. Fortuitously, on account of circuit symmetry, this

distribution is equal and opposite to the distribution of the acceleration force F_a.

III. SEAT OF THE RECOIL FORCE

Identifying the seat of the recoil force in a railgun structure is a perplexing issue. There should be some way in which the projectile can communicate with the branch of the circuit in which the recoil arises. The medium of communication should be the magnetic field. Railguns can be very long and the magnetic field generated at the breach by the current in the projectile will always be very small. It is this weak field which must transfer the strong recoil equal to the acceleration force. Besides, if the reaction force is experienced by the source of the magnetic field, it should appear in the rails close to the projectile. But the Lorentz force on the rails does not possess a component that could react to the acceleration force. The transmission of the recoil force *through* the nonuniform magnetic field of a long accelerator does not seem to be a defensible argument.

The Ampere force law, Eq. (2), predicts that the recoil force has its seat in the rails, and most of it is located quite close to the projectile. The Ampere recoil arises from the current-element repulsion across the corners of the circuit, as indicated in Fig. 3. The current element m of the projectile branch p repels the current-element n of rail s, because $\cos\epsilon = 0$ and $\cos\beta$ is negative. The transverse component of the repulsion of m is the acceleration force ΔF_a, while the longitudinal component of the repulsion force on n is the corresponding recoil force. This holds for any current-element combination between projectile and rails. Ampere[10] proved with a series of classical experiments that longitudinal forces do indeed exist, and he demonstrated them directly by the experiment described on p. 329 of Ref. 10. F. E. Neumann,[11] who explained electromagnetic induction on the basis of Ampere's force law, gave classroom demonstrations of the action of longitudinal forces. Early in the present century, Hering[12] built liquid metal pumps (without magnets) running on longitudinal forces. The author recently discovered electromagnetic jet propulsion in the direction of current flow between solid and liquid conductors.[13] These facts provided the incentive for an experimental test of longitudinal recoil forces in the railgun geometry.

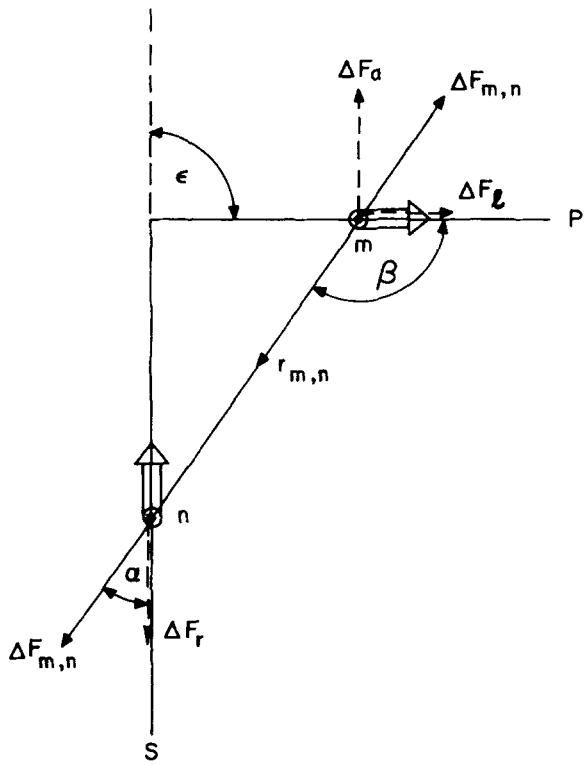

FIG. 3. Ampere recoil force ΔF_r between a current element in the projectile branch p and another element in rail s.

IV. RECOIL EXPERIMENT

Currents of a few hundred amperes are sufficient to generate acceleration and recoil forces of the order of a few grams. This is enough to move submerged copper cylinders along mercury troughs.[13] Experiments of this kind are simple, require little equipment, and permit close observation of dynamic events without excessive Joule heating.

Figure 4 is a photograph of the experimental setup. Rails of 45.72 cm length and 1.27-cm square cross section were spaced with 1.27 cm between them. The first 30.48 cm of each rail consisted of a copper bar and the remainder up to the projectile branch was liquid mercury contained in rectangular grooves that had been milled into a thick transparent plastic board. The *fixed* projectile was a 1.27-cm square copper bar set into the same board and being 3×1.27 cm long to fully bridge the gap between the mercury rails. At the other end, the rails were connected to a power supply with which dc currents up to 450 A could be passed through the circuit.

Right circular copper cylinders of 5 cm length, tinned overall for easy amalgamation with mercury, were placed on the mercury surfaces with one end of the cylinders touching the projectile branch, as indicated by Fig. 4(a). While they were lying on the surface, the copper rods were found to stick quite firmly to the mercury because of surface tension effects. But above certain currents, the rods would submerge and then much of the resistance to motion apparently disappeared. Experiments were carried out with three rod diameters of 0.300, 0.196, and 0.127 cm. The corresponding submersion currents in the rails were approximately 280, 240, and 140 A. On turning the current off one second or less after submersion, the copper rods would surface some distance away from the projectile branch, as shown by Fig. 4(b). This distance through which the rods traveled along the rails was a function of rail current, cylinder diameter, and time of current flow. With 0.196-cm-diam rods, longitudinal displacements of the order of two to three centimeters were observed after having forced a current of 450 A to flow for less than one second. This longitudinal displacement is believed to be caused by the force which, in a railgun, would be responsible for the recoil.

Submersion is the result of current sharing between copper rods and mercury and the lateral attraction of parallel currents. Both Eqs. (2) and (3) require this behavior. A working formula derived from Eq. (3) for the attraction between two straight, finite-length current filaments is[14]

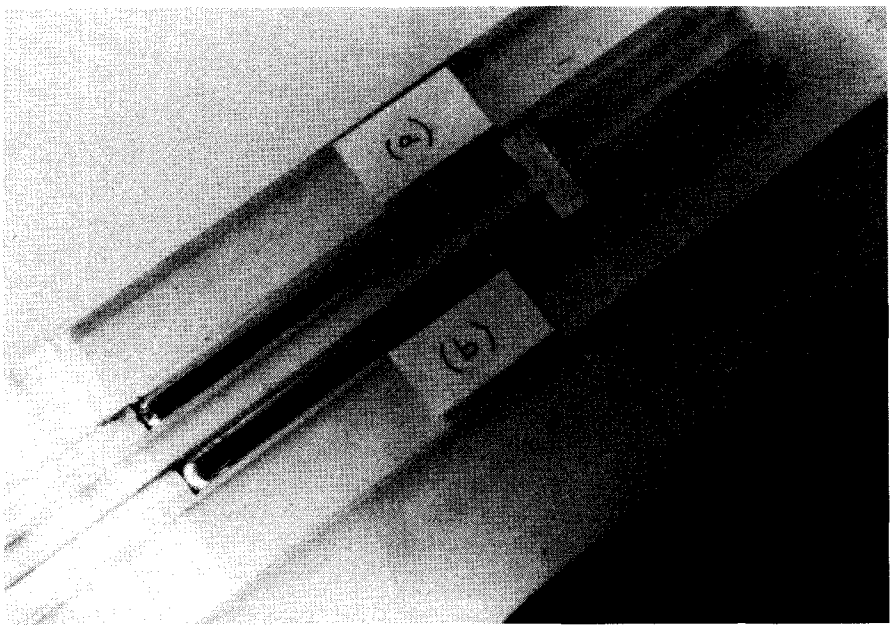

FIG. 4. Photograph of mercury troughs and short copper rods used in connection with the recoil force experiment.

$$F = 2i_1 i_2 \ell[(1/d) - (1/\ell)] \quad \text{dyn}, \tag{5}$$

where i_1 and i_2 are the two currents in absolute ampere A_{ab}, d (cm) the distance between the center lines, and ℓ(cm) the length of the filaments. Equation (5) may be used to calculate the centering force F_c acting on the copper rod. For this purpose the channel cross section has to be subdivided into a number of filaments sized such that one of them may represent the copper rod. Equation (5) then has to be applied to the rod and each mercury filament in turn. Figure 5 shows the force balance on the copper rod resulting from the centering force F_c, the buoyancy force F_b, and the transverse force F_t due to the current in the second rail. For any given rail current, the copper rod will come to rest at a different equilibrium position. For increasing rod diameter, the current fraction in the copper will also increase and thereby reduce the centering force. Finally, the rod may be driven against the trough wall without being pulled below the liquid surface. Under these circumstances, any longitudinal force acting on the cylinder has to overcome wall adhesion in addition to viscous drag. This was observed with the 0.3-cm-diam rods, which showed shorter longitudinal recoil displacements than the two smaller rod sizes.

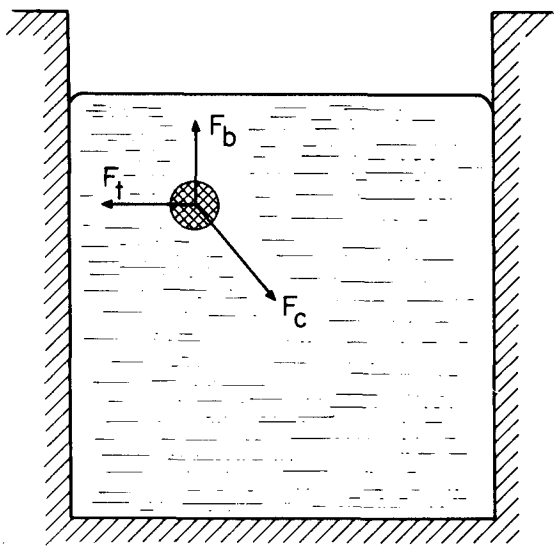

FIG. 5. Forces acting on the copper cylinder while it is submerged in the mercury trough.

According to Ampere's force law the copper cylinders should also be repelled from the solid rail sections at the other two ends of the mercury troughs. Experiment confirmed this. However, in a railgun without liquid metal portions, this latter repulsion would be taken up by a strain in the metal lattice and could not contribute to the recoil mechanism.

V. FINITE CURRENT-ELEMENT ANALYSIS

Equation (1) gives the reaction force between two parts of a current carrying circuit, but it is not suitable for calculating the force distribution. As this distribution is important information for the design of railgun structures, we have to resort to either Eq. (2) or (4).

It will be realized from Fig. 3 that the Ampere law not only places the recoil force in the rails but also predicts the action of longitudinal forces ΔF_ℓ in the projectile branch. The transverse force distributions given by Eqs. (2) and (4) and the longitudinal Ampere force distributions have been computed by finite current-element analysis for a conveniently sized circuit on which the specific acceleration force could be measured.

The dimensions of the analyzed circuit are indicated in Fig. 1. They were chosen for the experimental check to be described later and not with any particular accelerator application in mind. The circuit was built of 1.27 cm wide and 0.127 cm thick copper strip, making the rail height h equal to the strip width of 1.27 cm. The results of the finite current-element analysis actually apply to any scaled system in which the ratios of rail length:p-branch length:rail height are

787:236:10. For the purpose of delineating an element size, the strip was subdivided into ten square-section parallel filaments, and each element was then taken to be a cube of 0.127-cm sides. This resulted in a total of 20 460 current elements.

Computers were employed to apply Eqs. (2) and (4) to pairs of current elements in succession and sum the component forces in order to obtain both the force distributions plotted in Figs. 6 and 7 and the specific forces listed in Table I. It will be seen from the table that the specific acceleration forces F_a/i^2 predicted by Ampere's and Grassmann's formulas agree quite closely. The distributions of this force, shown in Fig. 7, are also in good agreement, although not identical. Moving the rails closer together would make this distribution more uniform with less concentration of force at the ends of the projectile branch. But this entails a reduction in the total specific acceleration force. Practical railguns with a square bore, in which the rail height is equal to the rail spacing, may have a specific acceleration force of only one-quarter of that calculated for the geometry of Fig. 1.

As can be seen from Fig. 6, the longitudinal Ampere forces are also concentrated at the corners of the circuit, just like the transverse forces. The recoil force listed in Table I for one rail is a little less than half the acceleration force, indicating that a very small fraction of the recoil has its seat in the breach of the railgun. The compressive buckling forces in the p branch listed in Table I are almost as large as the recoil and therefore of practical significance.

To appreciate the demands which the Ampere recoil force makes on rail strength, consider an example in which all linear dimensions of the circuit of Fig. 1 are multiplied by a factor of 10. The rail cross section would then be 12.7×1.27 cm. Assuming an operating current density of 7750 A/cm^2, the rail current comes to 125 000 A = 12 500 A_{ab}. This leads to a recoil force per rail of 685 kg, which is capable of buckling a copper strut of the specified dimensions, provided the force persists for a sufficient period of time. Hence experiments with large railguns should provide another check on the contention made by Ampere's force

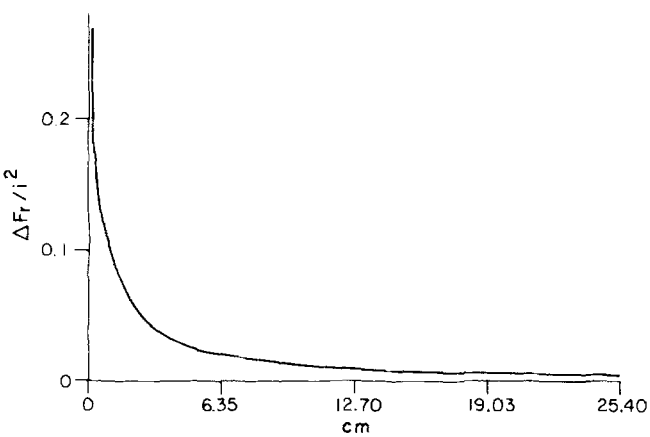

FIG. 6. Ampere recoil-force distribution along the first 200 current elements (25.4 cm) of one rail of the circuit of Fig. 1. The origin represents the point of contact between rail and projectile branch.

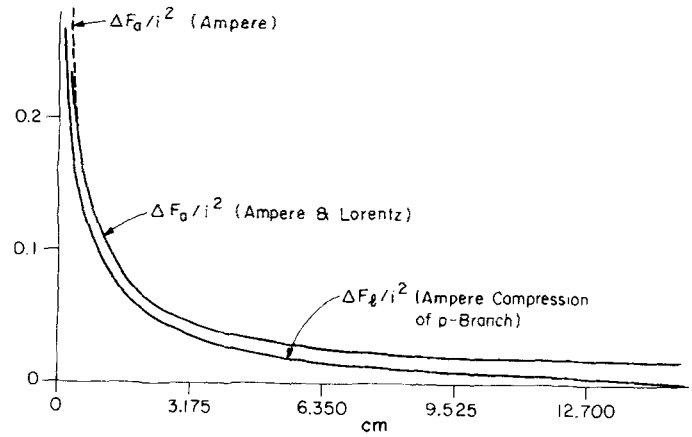

FIG. 7. The distribution of the acceleration force and strut compression force across half of the length of the projectile branch.

law regarding the seat of the recoil force. Furthermore, the Ampere electrodynamics imply that railgun accelerators would not work well with liquid metal or plasma rails because much of the energy would then produce fluid motion rather than projectile acceleration.

VI. ACCELERATION FORCE MEASUREMENTS

Publications referring to the measurement of reaction forces between parts of a current carrying circuit are very rare. It therefore seemed desirable to confirm the accuracy of the finite-element calculations by experiment. The technique used for this purpose may be described as force weighing and was originally outlined by Roper.[15] Figure 8 is a photograph of the force balance arrangement. Rails and breach were mounted on a vertical board. The lower ends of the rails were allowed to dip into nonmetallic cups attached to the projectile branch of the circuit and containing liquid mercury. The projectile branch was hung from one side of a commercial beam balance with a sensitivity of 0.1 gm. But for the 0.1 cm long liquid mercury gaps, the circuit consisted of the 1.27 cm wide and 0.127 cm thick copper strip bent sharply at both the top corners and the entrance of the power supply leads.

Currents of up to 450 A were passed around the circuit for short periods of time (less than one minute) to establish the downward-directed acceleration force as a function of current. The conductor was allowed to cool down between measurements, and its temperature was kept below 50 °C to prevent noticeable thermal expansion. The beam swing of

TABLE I. Computed and measured forces.

	Specific acceleration force (F_a/i^2)	Specific recoil (one rail) (F_r/i^2)	Specific compression (p branch) (F_ℓ/i^2)
Ampere-Law [Eq. (2)]	9.403	4.695	4.444
Grassmann-Law [Eq. (4)]	9.268	...	...
Experiment	9.76		

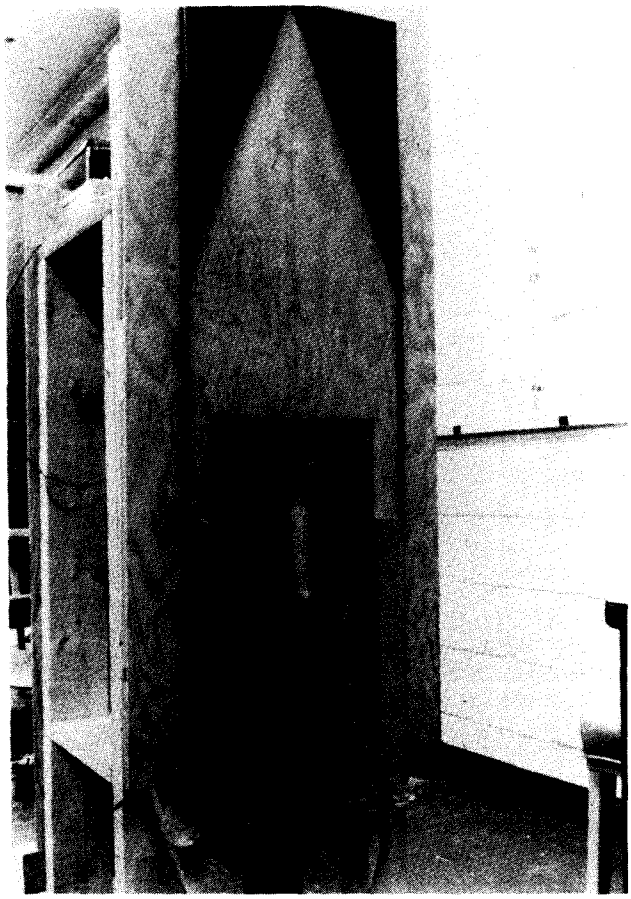

FIG. 8. Photograph of force weighing setup.

the balance was severely restricted with mechanical stops to keep buoyancy variations in the mercury cups down to negligible amounts.

The results of the meausrements are plotted in Fig. 9. Agreement between the measurement points and the calculated straight line is seen to be good. All experimental points should lie slightly above graph (2), representing Ampere's force law, and graph (1), representing the Lorentz force law, because the pinch-force thrust F_p in the mercury cups has not been taken into account in the finite current-element analysis. Figure 10 shows the mercury cups in greater detail. Standard pinch-force theory, first developed by Northrup,[16] shows this effect to be independent of the conductor cross section and given by

$$F_p/i^2 = 0.5 \tag{6}$$

per liquid gap. This should add 1.00 to the theoretical acceleration forces listed in Table I and would boost the force above the measured force by the amount indicated by graph (3) in Fig. 9.

VII. DISCUSSION AND CONCLUSIONS

As electrodynamic forces between current elements fall off as the square of distance, it seems unnatural that the strong recoil forces of a railgun accelerator should make themselves felt in the branch of the circuit that lies furthest away from the projectile. This doubt has also been expressed by other investigators[17–19] who studied reaction forces between parts of rectangular circuits. Ampere's force law, Eq. (2), gives a more credible result by placing the seats of the recoil forces into the railheads adjacent to both ends of the projectile branch. They must then be forces acting along the streamlines of current flow. Ampere[10] himself, as well as F. E. Neumann,[11] Hering,[12] and Graneau,[13] have reported experiments which confirm the existence of longitudinal mechanical forces of electromagnetic origin. A further experiment described in the present paper furnishes direct evidence of a longitudinal recoil mechanism. It should also be remembered that after 160 years, there is still no experiment on record which demonstrates Ampere's force law to be wrong when applied to metallic circuits.

It has been known for a long time, and established analytically, that both force laws, Eqs. (2) and (3), agree identically on the reaction force between two closed circuits and also the Lorentz force distribution on either circuit due to the current in the other. Yet, there exists no analytical proof that both laws give the same transverse force distribution on an isolated current carrying circuit, regardless of the shape of the circuit. The analytical difficulties have to do with singularities in the integral of the interaction forces. The finite current-element analysis described in this paper avoids the singularities by forbidding the self-interaction of individual current elements. For the geometry under consideration, the finite-element method gives almost identical transverse force distributions with both Ampere's and the Biot-Savart-Lorentz force law. This is remarkable in view of the different predictions the two equations make with regard to longitudinal forces.

Longitudinal Ampere forces reveal not only an unexpected recoil mechanism, but they also suggest that the projectile branch is being stressed like a strut in compression. The recoil forces should be capable of buckling copper rails unless the rails are suitably reinforced.

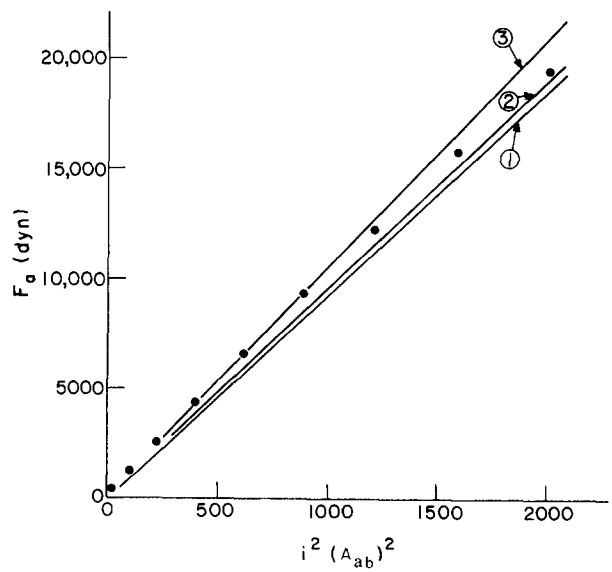

FIG. 9. Measured and computed acceleration forces. (1) Grassmann formula [Eq. (4)]; (2) Ampere formula [Eq. (2)]; (3) Ampere formula plus pinch thrust of Eq. (6).

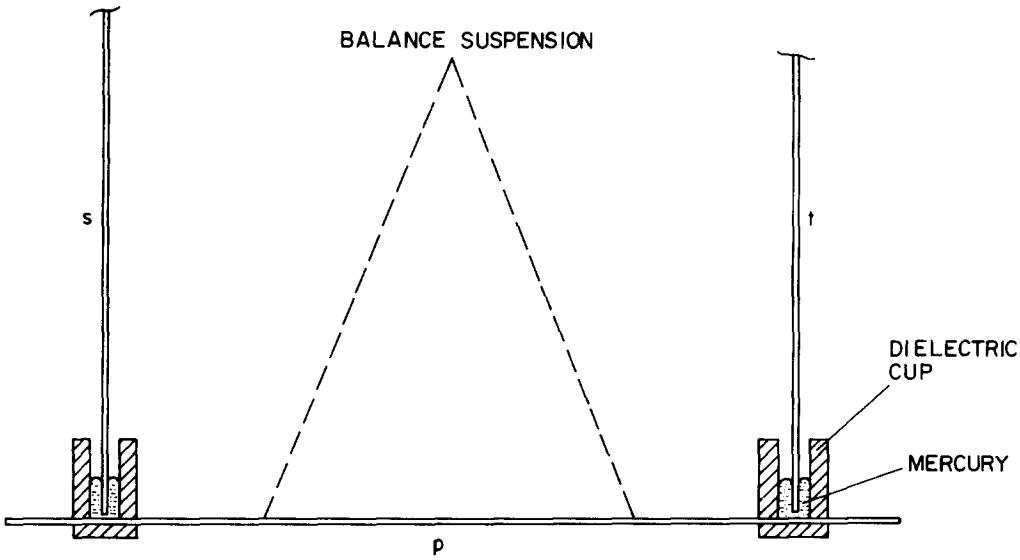

FIG. 10. Mercury cup details.

The broad conclusion drawn from this investigation is that Ampere's law correctly describes the distribution of mechanical forces of electromagnetic origin around the railgun circuit. It supports the intuitive notion of the recoil force residing in the railheads right adjacent to the accelerating projectile. Both laws give very nearly the same acceleration force, and they also agree on the distribution of this force. But the Ampere law predicts an additional compressive force to be found in the projectile branch which does not conform with the Lorentz force concept. In liquid metal and plasma conductors, the longitudinal Ampere forces are likely to produce fluid motion, wasting some of the energy which would otherwise be available for projectile acceleration.

ACKNOWLEDGMENTS

This research was supported by Grant No. ECS-8012995 from the National Science Foundation.

Whitney Hamnet built the experimental apparatus and Neal Graneau was responsible for computer programming.

[1]D. Brast and D. Sawle, NASA Report No. NAS-8-11204, 1965.
[2]S. Rashleigh and R. Marshall, J. Appl. Phys. **49**, 2540 (1978).
[3]R. S. Hawke and J. K. Scudder, *Megagauss Physics and Technology*, edited by P. Turchi (Plenum, New York, 1980), p. 297.
[4]R. S. Hawke, IEEE Trans. Nucl. Sci. **NS-28**, 1542 (1981).
[5]I. R. McNab, J. Appl. Phys. **51**, 2549 (1980).
[6]H. B. Dwight, Trans. AIEE **46**, 570 (1927).
[7]W. E. Smith, Austr. J. Phys. **18**, 195 (1965).
[8]J. C. Maxwell, *A Treatise on Electricity and Magnetism* (Oxford University, New York, 1873), Vol. 2, p. 318.
[9]H. H. Grassmann, Poggendorf's Annalen der Physik und Chemi **64**, 1 (1845).
[10]A. M. Ampere, *Memoires sur l'electrodynamic*, XXV (Gauthier-Villars, Paris, 1885), Vol. 1, p. 329.
[11]F. E. Neumann, *Vorlesungen ueber elektrische Stroeme* (Teubner, Leipzig, 1884), p. 102.
[12]C. Hering, J. Franklin Inst. **194**, 611 (1921).
[13]P. Graneau, Nature **295**, 311 (1982).
[14]B. Hague, *The Principles of Electromagnetism Applied to Electrical Machines* (Dover, New York, 1962) p. 327.
[15]J. W. Roper, J. AIEE **46**, 913 (1927).
[16]E. F. Northrup, Phys. Rev. **24**, 474 (1907).
[17]F. F. Cleveland, Philos. Mag. **25**, 416 (1936).
[18]A. O'Rahilly, *Electromagnetic Theory* (Dover, New York, 1965), Vol. 1, p. 102.
[19]I. A. Robertson, Philos. Mag. **36**, 32 (1945).